

■ Grignard Reagents | *Hot Paper* |**Association and Dissociation of Grignard Reagents RMgCl and Their Turbo Variant $\text{RMgCl}\cdot\text{LiCl}$** Christoph Schnegelsberg,^[a] Sebastian Bachmann,^[b] Marlene Kolter,^[a] Thomas Auth,^[a] Michael John,^[a] Dietmar Stalke,^[b] and Konrad Koszinowski*^[a]

Abstract: Grignard reagents RMgCl and their so-called turbo variant, the highly reactive RMgCl-LiCl, are of exceptional synthetic utility. Nevertheless, it is still not fully understood which species these compounds form in solution and, in particular, in which way LiCl exerts its reactivity-enhancing effect. A combination of electrospray-ionization mass spectrometry, electrical conductivity measurements, NMR spectroscopy (including diffusion-ordered spectroscopy), and quantum chemical calculations is used to analyze solutions of RMgCl (R = Me, Et, Bu, Hex, Oct, Dec, *i*Pr, *t*Bu, Ph) in tetrahydrofuran and other ethereal solvents in the absence and presence of stoichiometric amounts of LiCl. In tetrahydrofuran, RMgCl forms mononuclear species, which are converted

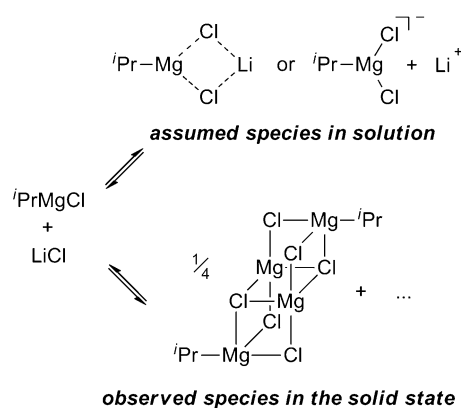
into trinuclear anions as a result of the concentration increase experienced during the electrospray process. These trinuclear anions are theoretically predicted to adopt open cubic geometries, which remarkably resemble structural motifs previously found in the solid state. The molecular constituents of RMgCl and RMgCl-LiCl are interrelated via Schlenk equilibria and fast intermolecular exchange processes. A small portion of the Grignard reagent also forms anionic ate complexes in solution. The abundance of these more electron-rich and hence supposedly more nucleophilic ate complexes strongly increases upon the addition of LiCl, thus rationalizing its beneficial effect on the reactivity of Grignard reagents.

Introduction

Since their discovery by Grignard in the year of 1900,^[1] the organomagnesium halides RMgX that bear his name have been known and cherished as *the* prototypical organometallic reagents.^[2] Grignard reagents not only react readily with numerous electrophiles, such as aldehydes, ketones, epoxides, nitriles, esters, and carbon dioxide,^[3,4] but also efficiently undergo transition metal-catalyzed conjugate addition^[5] and cross-coupling reactions.^[6] Thus, they are indispensable tools for the formation of new carbon-carbon bonds and continue to attract a great deal of interest. Important milestones in the development of Grignard reagents include the activation of the magnesium metal for a more facile access to RMgX compounds^[7] and the synthesis and use of highly functionalized Grignard reagents.^[8] The latest pivotal innovation is marked by the development of the so-called turbo-Grignard reagent *i*PrMgCl-LiCl by Knochel and co-workers.^[9] The presence of LiCl strongly enhances the reactivity of this reagent and, thus, enables highly efficient magnesium-bromine exchange reactions. Thereby, it further broadens the scope of accessible polyfunctionalized Grignard reagents. Thanks to their superior performance, *i*PrMgCl-LiCl and other LiCl-containing Grignard reagents are by now widely adopted in academia^[10] and industry.^[11] At the same time, the addition of LiCl also significantly accelerates the insertion of magnesium into organic halides.^[12] RMgCl-LiCl reagents, thus, represent a prime example of the emergence of synergistic effects in the reactivity of bimetallic main-group compounds.^[13]

The outstanding synthetic utility of Grignard reagents has always resulted in a keen interest in their speciation in solution. The classical studies by Schlenk and Schlenk showed that Grignard reagents RMgX in ethereal solutions undergo disproportionation to afford both R₂Mg and MgX₂ (the so-called Schlenk equilibrium).^[14] Later work of Ashby and others used ebullioscopy and kinetic measurements as well as NMR, IR, and X-ray absorption spectroscopy to determine the position of the Schlenk equilibria and the aggregation state of RMgX.^[15,16] These studies pointed to the presence of monomeric and dimeric RMgX in diethyl ether. In tetrahydrofuran (THF), only monomeric species were found, but here the operation of the Schlenk equilibrium is more pronounced and gives rise to the formation of substantial amounts of R₂Mg and MgX₂, besides RMgX. Electrochemical experiments also indicated the presence of ionic species, although only in low abundance.^[17] The nature of these ionic species remains unclear.

More recent studies have also addressed the microscopic constitution of turbo-Grignard reagents. Krasovskiy and Knochel suggested that the addition of LiCl to RMgCl in THF may lead to ate complexes, which should exhibit an enhanced nucleophilic reactivity (Scheme 1, top left).^[9a] Quantum-chemical calculations by Krasovskiy, Straub, and Knochel confirmed the



Scheme 1. Constituents of *i*PrMgCl-LiCl assumed to be present in solution (THF)^[9a,18] and found in the solid state,^[19] respectively. Coordinating solvent molecules are omitted for clarity.

[a] C. Schnegelsberg, M. Kolter, T. Auth, Dr. M. John, Prof. Dr. K. Koszinowski
Institut für Organische und Biomolekulare Chemie
Georg-August-Universität Göttingen
Tammannstraße 2, 37077 Göttingen (Germany)
E-mail: konrad.koszinowski@chemie.uni-goettingen.de

[b] S. Bachmann, Prof. Dr. D. Stalke
Institut für Anorganische Chemie
Georg-August-Universität Göttingen
Tammannstraße 4, 37077 Göttingen (Germany)

Supporting information for this article is available on the WWW under <http://dx.doi.org/10.1002/chem.201600699>.

assumed correlation between ate character and nucleophilic reactivity.^[18] In the same study, the authors also found evidence for the operation of Schlenk equilibria and the formation of solvent-separated ion pairs from the ate complex and its Li^+ counter ion (Scheme 1, top right).^[18] Such ion pairs were not observed in crystals isolated from solutions of *i*PrMgCl·LiCl, however. Instead, Lerner and collaborators found these crystals to display neutral open-cube geometries of four Mg centers without the incorporation of Li (Scheme 1, bottom).^[19] The same structure was obtained for crystals isolated from the corresponding conventional Grignard reagent *i*PrMgCl.^[19,20]

To elucidate the effect of LiCl upon Grignard reagents at the molecular level, the direct identification of the in situ-formed species by spectrometric and spectroscopic methods is essential. Herein, we analyze solutions of conventional Grignard reagents RMgCl and their turbo variant RMgCl·LiCl in THF by a combination of electrospray-ionization (ESI) mass spectrometry, electrical conductivity measurements, and multinuclear NMR spectroscopy, including diffusion-ordered spectroscopy (DOSY). ESI mass spectrometry selectively probes charged species and, thus, is very well suited to detect anionic ate complexes, as we and others have shown previously.^[21,22] Note, however, that the notoriously high sensitivity of Grignard reagents toward hydrolysis and oxidation so far has prevented the successful detection of intact organomagnesium species by ESI mass spectrometry.^[23,24] The analysis of these challenging analytes therefore also serves as a rigorous test for the applied methods. The qualitative insight afforded by ESI mass spectrometry is ideally complemented by electrical conductivity measurements, which can provide more quantitative information on the ionic constituents in solution.^[21b,c,25] NMR spectroscopy, in turn, has the advantage of probing both neutral and charged species. Moreover, its DOSY variant can be used to determine the aggregation state of the sampled species, which is particularly helpful for the characterization of organometallics and metal bases in solution.^[26] However, one drawback of NMR spectroscopic experiments is their relatively slow time scale, which prevents the resolution of fast equilibria. To facilitate the interpretation of the experimental results, we also employ quantum chemical calculations.

Experimental and Theoretical Methods

Materials and general methods

Standard Schlenk techniques were applied in all cases. THF and $[\text{D}_8]\text{THF}$ were dried over sodium or potassium/benzophenone and freshly distilled before use. Et_2O was dried over sodium and freshly distilled. Dioxane was freshly distilled and degassed. MeMgCl (in THF, 3 M), EtMgCl (in THF, 2 M), and PhMgCl (in THF, 2 M) were purchased and used as received. BuMgCl, HexMgCl, OctMgCl, DecMgCl, *i*PrMgCl, and *t*BuMgCl were synthesized according to standard procedures (see the Supporting Information). Exact concentrations of the Grignard reagents were determined by iodometric titration.^[27] Solutions of RMgCl·LiCl were prepared by combining equimolar amounts of solutions of RMgCl and dry LiCl in THF.

ESI mass spectrometry

Before the analysis of solutions of Grignard reagents, the inlet line of the mass spectrometer was extensively purged with dry THF. Sample solutions ($c=25\text{ mM}$ if not stated otherwise) were then transferred into gas-tight syringes and injected into the ESI source of an HCT quadrupole-ion trap mass spectrometer (Bruker Daltonik) at a flow rate of $8\ \mu\text{L}\cdot\text{min}^{-1}$. The ESI source was operated at a voltage of $\pm 3000\text{ V}$ with N_2 as nebulizer gas (0.7 bar) and drying gas ($5.0\text{ L}\cdot\text{min}^{-1}$, 373 K). To transfer the generated ions into the quadrupole-ion trap, very mild conditions were applied to prevent unwanted decomposition reactions.^[21b,28] The helium-filled trap [estimated pressure $p(\text{He})\approx 0.3\text{ Pa}$] was typically operated at a trap drive of 40 to ensure efficient trapping and detection of ions of medium m/z ratios (typically recorded m/z range: 50–1000). The given assignments are based on the m/z ratios, the isotope patterns (some of which were significantly broadened and, thus, poorly resolved, presumably due to reactions with traces of background water during the m/z scan), and the gas-phase fragmentation behavior of the observed ions. In the gas-phase fragmentation experiments, the ions of interest were mass-selected (with isolation widths of 8 u), subjected to excitation voltages of amplitude V_{excr} and allowed to collide with the helium gas. Additional experiments were carried out with a micrOTOF-Q II mass spectrometer (Bruker Daltonik) under similar ESI conditions.^[29] This instrument is equipped with a time-of-flight mass analyzer and, thus, achieves a higher mass resolution than the quadrupole-ion trap (typically, deviations of 20 ppm were obtained when the instrument was externally calibrated with a mixture of phosphazenes in $\text{H}_2\text{O}/\text{acetonitrile}$). A drawback of the micrOTOF-Q II instrument is the imperfect insulation of its ESI source against the surrounding atmosphere and the resulting intake of trace amounts of water and oxygen. Both instruments were controlled with the Compass software package (Bruker Daltonik), which was also used to calculate exact m/z ratios and theoretical isotope patterns.

Electrical conductivity measurements

Electrical conductivity experiments were performed with a Seven Multi instrument (Mettler Toledo) with a stainless steel electrode cell ($\kappa_{\text{cell}}=0.1\text{ cm}^{-1}$, calibrated against an aqueous solution of KCl at 298 K) at $T=298\pm 1\text{ K}$. Iodometric titration immediately after each measurement proved that the sample solutions still had $\geq 90\%$ of the expected activity.

NMR spectroscopy

Samples of RMgCl or RMgCl·LiCl ($c=25\text{ mM}$) and equimolar amounts of 1,2,3,4-tetraphenylnaphthalene (TPhN) were filled into 5 mm NMR tubes and kept inside the NMR spectrometer at 298 K for 30 min (with an air flow of $400\text{ L}\cdot\text{h}^{-1}$) before the measurement, if not stated otherwise. All experiments were performed with a Bruker Avance 400 spectrometer equipped with an observe broadband probe with a z-axis gradient coil with a maximum gradient strength of $57\text{ G}\cdot\text{cm}^{-1}$ and without sample spinning during measurements. The DOSY experiments employed a double stimulated echo sequence with bipolar gradient pulses and three spoil gradients with convection compensation (dstebpg3s).^[30] The diffusion time was set to $\Delta=0.1\text{ s}$. The pulsed field gradients $\delta/2$ were adjusted for every compound in a range of 2–3 ms. The delay for gradient recovery was 0.2 ms and the eddy current delay 5 ms. For each DOSY experiment, a series of 16 spectra on 32 K data points was collected. The pulse gradients (g) were incremented from 2 to 98% of the maximum gradient strength in a linear ramp with

a total time of the experiment of 51 min. After Fourier transformation and baseline correction, the diffusion dimension was processed with the Topspin 3.1 software (Bruker Biospin). Diffusion coefficients processed with a line broadening of 2 Hz were calculated by exponential fits with the T1/T2 software of Topspin.

Quantum chemical calculations

Electronic structure calculations were performed with the ORCA program package (version 3.0.3).^[31,32] The presented gas-phase minimum energy structures were calculated without any constraints by the DFT method B3LYP^[33] (as defined in the GAUSSIAN program system) in combination with Grimme's atom-pairwise dispersion correction with Becke–Johnson damping (DFT-D3bj).^[34] For all atoms, the def2-TZVP basis set^[35] minimally augmented (ma) by diffuse functions according to Truhlar and co-workers^[36] was applied. To obtain minimum energy geometries in solution, the same method was used together with the conductor-like screening model COSMO.^[37] All optimized structures were confirmed to correspond to a minimum in energy by means of harmonic vibrational frequency calculations (conducted at the same level of theory as each geometry optimization).

Results

ESI mass spectrometry

RMgCl in the absence of LiCl

Upon analysis by negative ion-mode ESI mass spectrometry, solutions of Grignard reagents RMgCl bearing primary alkyl groups (R=Me, Et, Bu, Hex, Oct, Dec) showed a multitude of organomagnesium ate complexes (Figure 1; Figures S1–S19 and Table S1 in the Supporting Information). In all cases,

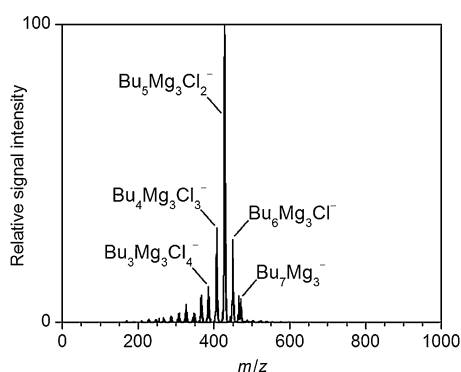


Figure 1. Negative ion-mode ESI mass spectrum of a 25 mM solution of BuMgCl in THF.

almost exclusively trinuclear anions of the type $[R_nMg_3Cl_{7-n}]^-$ were observed. Variation of the concentration of the sample solution did not change this result (see the Supporting Information, Figure S7). For Grignard reagents with short and medium alkyl chains (R=Me, Et, Bu, Hex), alkyl-rich complexes $[R_nMg_3Cl_{7-n}]^-$ ($n \geq 4$) predominated, whereas more balanced distributions were found for Grignard reagents with long alkyl substituents (R=Oct, Dec). It is not clear whether this trend reflects a genuine difference in behavior or whether it merely re-

sulted from the unavoidable mass discrimination inherent in the employed mass analyzer. Note that we succeeded in suppressing hydrolysis reactions essentially completely for some systems (e.g., for BuMgCl; Figure 1), whereas in other cases the observation of $[R_nMg_3Cl_{6-n}(OH)]^-$ and $[R_nMg_3Cl_{5-n}(OH)_2]^-$ complexes point to the partial occurrence of these unwanted processes.

Solutions of *i*PrMgCl and *t*BuMgCl also afforded prominent trinuclear ate complexes of the type $[R_nMg_3Cl_{7-n}]^-$, namely $[iPr_5Mg_3Cl_2]^-$ and $[tBu_3Mg_3Cl_4]^-$, respectively (see the Supporting Information, Figures S20–S24). Additional ions contained alkoxy groups, which presumably resulted from reactions with traces of dioxygen and the consecutive cleavage of the O-OR bonds by the nucleophilic attack of metal-bound R groups.^[15c,23c,38] Control experiments with sample solutions deliberately exposed to O₂ indeed found a dramatic increase of alkoxy complexes (see the Supporting Information, Figures S25 and S26).

The negative ion-mode ESI mass spectra of solutions of PhMgCl showed the trinuclear complex $[Ph_3Mg_3Cl_4]^-$ as base peak (see the Supporting Information, Figures S27–S29). In addition, the presence of di- and trinuclear ions with up to four hydroxy groups indicated extensive hydrolysis reactions.

We also analyzed a 1:1 mixture of *i*PrMgCl and PhMgCl in THF. The resulting ESI mass spectra indicated a series of trinuclear ate complexes, several of which contained both *i*Pr and Ph groups (see the Supporting Information, Figures S30–S32). The distribution of the two organic substituents in the detected anions was not statistical, but showed a significant enrichment in the *i*Pr group.

The analysis of solutions of Grignard reagents RMgCl by positive ion-mode ESI mass spectrometry only led to the observation of $[Mg_3Cl_3(OMe)_2(THF)_n]^+$ ions ($n=3-5$). As reported previously, these ions originated from reactions with surprisingly long-lasting MeOH contaminations present in the ESI source.^[23c]

RMgCl·LiCl

Negative ion-mode ESI of solutions of turbo-type Grignard reagents RMgCl·LiCl (R=Me, Et, Bu, Hex, Oct, Dec, *i*Pr, *t*Bu, Ph) gave mass spectra very similar to those obtained for the solutions of the corresponding conventional Grignard reagents RMgCl (see the Supporting Information, Figures S33–S43). Only for DecMgCl and PhMgCl, a few Li⁺-containing ions, such as $[Dec_6LiMg_3Cl_2]^-$ and $[PhMg_2LiCl_2(OH)_3]^-$, could be detected (see the Supporting Information, Figures S39, S40, and S43). Positive ion-mode ESI produced $[Li(THF)_n]^+$ ($n=2, 3$; see the Supporting Information, Figure S44 for BuMgCl·LiCl).

Effects of solvents and additives

Negative ion-mode ESI mass spectrometry of a solution of *i*PrMgCl in Et₂O afforded $[iPr_4Mg_3Cl_3]^-$ as base peak (see the Supporting Information, Figures S45–S47). Upon addition of 10% dioxane to a solution of *i*PrMgCl in THF, $[iPr_5Mg_3Cl_2]^-$, $[iPr_4Mg_3(OiPr)_nCl_{1-n}]^-$ ($n=0$ and 1), as well as $[iPr_{11}Mg_3]^-$ were

observed (see the Supporting Information, Figures S48–S51). The latter ion is remarkable because it is the only pentanuclear complex detected, which moreover exclusively contains organic substituents.

Reactivity in solution

We also used negative ion-mode ESI mass spectrometry to analyze solutions of *i*PrMgCl·LiCl in THF/dioxane (9:1), to which 4-bromoanisole (ArBr) had been added. From synthetic studies, it is known that under these conditions bromine–magnesium exchange reactions occur.^[18] We could indeed observe the resulting intermediates $[\text{Ar}_4\text{Mg}_2\text{Cl}]^-$ and $[\text{Ar}_5\text{Mg}_2]^-$, which showed the complete replacement of all exchangeable *i*Pr groups by aryl substituents (Figure 2 and Figures S52 and S53 in the Supporting Information). Unlike the vast majority of other detected organomagnesium ate complexes, these species were dinuclear. In addition, the trinuclear anion $[\text{Ar}_4\text{Mg}_3(\text{O}i\text{Pr})_2\text{Cl}]^-$ was present and again pointed to the occurrence of reactions with traces of O_2 .

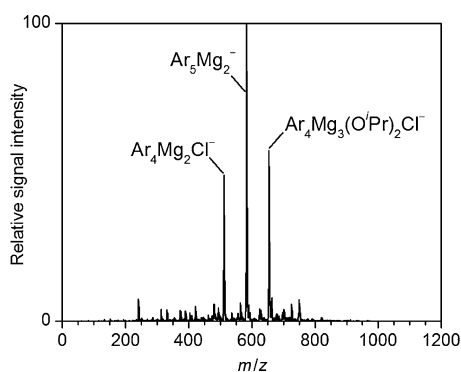
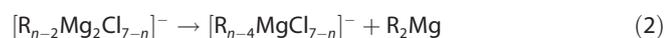
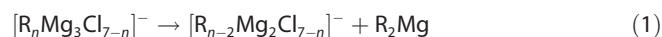


Figure 2. Negative ion-mode ESI mass spectrum of a solution of the products formed in the reaction of *i*PrMgCl·LiCl (25 mM) with 4-bromoanisole (ArBr, 25 mM) in THF/dioxane (9:1).

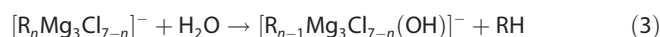
Gas-phase reactivity

In all cases examined,^[39] the gas-phase fragmentation of the organomagnesium ate complexes resulted in the loss of R_2Mg units [Eq. (1) and Table S2 and Figures S54–S75 in the Supporting Information]. In a few cases, the primary fragment ions underwent a consecutive fragmentation and lost another R_2Mg unit [Eq. (2) and Figures S76–S78 in the Supporting Information]. Analogous fragmentation reactions also occurred for the pentanuclear $[\text{iPr}_{11}\text{Mg}_5]^-$ ion (see the Supporting Information, Figure S79) and the lithium-containing complexes (see the Supporting Information, Figures S80 and S81).



These unimolecular reactions were partly obscured by the parallel occurrence of bimolecular reactions with traces of

water present in the vacuum system of the mass spectrometer, which led to the partial hydrolysis of the organomagnesium ate complexes [Eq. (3) for the case of the trinuclear ions]. The rates of these reactions apparently depended on the nature of the organic substituent and were particularly high for the phenylmagnesium ate complexes. For these species, multiple consecutive hydrolysis steps were observed (see the Supporting Information, Figures S82–S84).



Electrical conductivity measurements

RMgCl + *n* LiCl

Solutions of Grignard reagents *RMgCl* (*R*=Bu and *i*Pr) in THF displayed relatively low electrical conductivities (Figure 3). In contrast, the conductivity of a solution of *t*BuMgCl was markedly higher. Upon addition of 0.5–2 equivalents of LiCl, the conductivity significantly increased in all cases (Figure 3 and Tables S3 and S4). With the exception of the *i*PrMgCl/*n*LiCl system, the measured curves exhibited approximately linear slopes without any apparent signs of saturation. Note that the conductivity of LiCl in THF alone is negligibly low (see below) and, thus, cannot account for the observed increase.^[40]

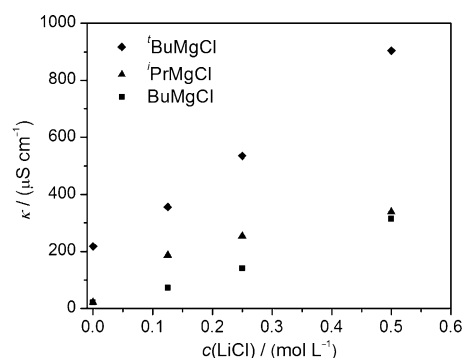


Figure 3. Specific electrical conductivities of solutions of *RMgCl* (approx. 250 mM) treated with different amounts of LiCl in THF at 298 K.

BuMgCl/LiCl: Job plot

To obtain complementary information, we also employed the method of continuous variation, commonly known as a Job plot.^[41] To this end, we considered different binary mixtures of *BuMgCl* and LiCl in THF with a constant total concentration $c_{\text{total}} = c(\text{BuMgCl}) + c(\text{LiCl}) = 250 \text{ mM}$. Plotting the electrical conductivities of these mixtures against the molar fraction of *BuMgCl* resulted in a curve with a pronounced maximum at $x(\text{BuMgCl}) = 0.5$ (Figure 4). The curve showed a slightly asymmetric shape due to the different conductivities of the two pure components: that of LiCl was negligibly low,^[40] unlike that of *BuMgCl* (see above).

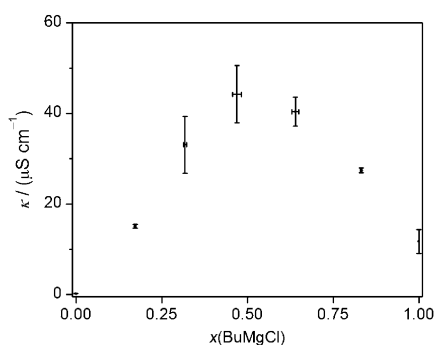


Figure 4. Job plot for a mixture of BuMgCl and LiCl in THF at 298 K, $c_{\text{total}} = 250 \text{ mM}$.

NMR Spectroscopy

RMgX in the absence of LiX

^1H and ^{13}C NMR spectra of Grignard reagents RMgCl ($R = \text{Et, Bu, Hex, Oct, Dec, } i\text{Pr}$) and of BuMgBr in $[\text{D}_8]\text{THF}$ showed the up-field-shifted signals characteristic of methylene or methine groups, respectively, directly bound to magnesium (Figure 5 and Figures S85–S113 in the Supporting Information). In all cases, a single set of signals was observed, suggesting the presence of only a single distinct species of BuMgCl or the operation of fast equilibria. Cooling down the sample to 193 K did not result in additional signals.

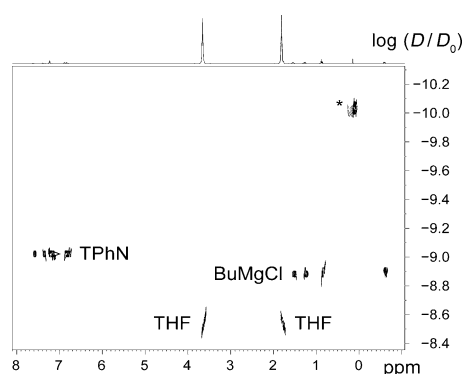


Figure 5. ^1H DOSY spectrum of a 25 mM solution of BuMgCl in $[\text{D}_8]\text{THF}$ at 298 K. TPhN = 1,2,3,4-tetraphenyl-naphthalene added as internal reference; the signal marked with an asterisk results from traces of grease.

Moreover, we used ^1H DOSY experiments to determine the diffusion coefficients of the organomagnesium species (Figure 5 and Figures S88, S92, S96, S100, S104, S108, and S113 in the Supporting Information). We assigned a fixed value to the diffusion coefficient of an internal reference (1,2,3,4-tetraphenyl-naphthalene; $\log D_{\text{ref,fix}} = -9.1054$) for all measurements and, thus, normalized all diffusion coefficients of the Grignard reagents. By using a carefully chosen external calibration curve (ECC; see the Supporting Information, Figure S114 and Tables S5–S9), we could convert these diffusion coefficients into molecular weights. These molecular weights showed a monotonous and evenly spaced increase with growing length of the

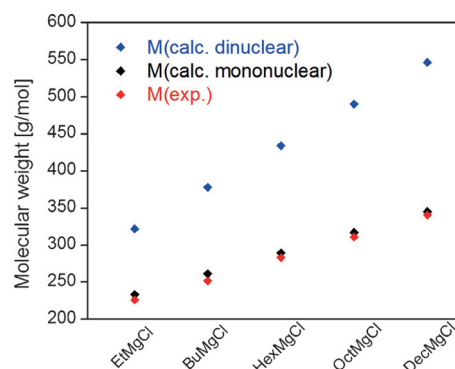


Figure 6. Comparison of experimentally derived molecular weights (red) with values expected for $[\text{RMgCl}(\text{THF})_2]$ (black) and $[\text{R}_2\text{Mg}_2\text{Cl}_2(\text{THF})_2]$ (blue).

alkyl chain of the Grignard reagents (Figure 6). This behavior strongly suggested that the probed compounds RMgCl belonged to a common series of homologous species. From the observed increase of the molecular weights per additional C_2H_4 unit in the alkyl chain, it can be directly deduced that the probed organomagnesium complexes contained exactly one alkyl group. The obtained molecular weights match those calculated for $[\text{RMgCl}(\text{THF})_2]$ very well (Figure 6). In contrast, assuming the presence of, for example, dinuclear $[\text{R}_2\text{Mg}_2\text{Cl}_2(\text{THF})_2]$ would not reproduce the derived molecular weights at all. In the case of BuMgCl, we also investigated the concentration dependence of the diffusion coefficient. A ten-fold concentration increase from 25 mM to 250 mM resulted in no significant increase of the diffusion coefficient. At $c = 1.0 \text{ M}$, the highest concentration that could be probed, the diffusion coefficient slightly increased. This behavior could indicate the partial formation of a higher aggregate interrelated to the $[\text{RMgCl}(\text{THF})_2]$ species via a fast equilibrium; the validity of the ECC DOSY method has, however, not been rigorously demonstrated for highly concentrated sample solutions.^[26g]

BuMgCl + LiCl

The addition of 1 equivalent of LiCl to solutions of BuMgCl had no discernible effects on the ^1H and ^{13}C NMR spectra (see the Supporting Information, Figures S115–S117). The ^7Li NMR spectra of the BuMgCl-LiCl solutions exhibited a signal at $\delta = 0.28 \text{ ppm}$, which slightly differed from the chemical shift of 0.49 ppm measured for solutions of LiCl (see the Supporting Information, Figure S118).

The ^1H DOSY experiments determined diffusion coefficients for BuMgCl-LiCl, which were consistently higher than those for simple BuMgCl (see the Supporting Information, Figure S119 and Table S10). This finding indicated that the addition of LiCl led to the (partial) association of the two components. The molecular weight deduced from the experiment ($MW_{\text{det}} \geq 299.6 \text{ g mol}^{-1}$)^[42] appears to agree with that calculated for a 1:1 adduct of BuMgCl-2THF and LiCl ($MW_{\text{calc}} = 303.5 \text{ g mol}^{-1}$) and to suggest that such species form almost quantitatively. If, instead, it is assumed that the adduct of the two components binds 3 molecules of THF, thus affording BuMgCl-LiCl-3THF

($MW_{\text{calc}} = 375.6 \text{ g mol}^{-1}$), the determined molecular weight implies its incomplete formation. In addition, we also studied solutions of BuMgBr-LiBr, whose NMR spectra closely resembled those of BuMgBr as well (see the Supporting Information, Figures S120–S124).

Quantum chemical calculations

Trinuclear ate complexes

For a better understanding of the almost exclusive formation of trinuclear ate complexes upon ESI of solutions of RMgCl and RMgCl-LiCl, we calculated the energetically most stable gas-phase structures of the model complexes $[\text{Mg}_3\text{Cl}_7]^-$ and $[\text{Me}_7\text{Mg}_3]^-$. Considering 12 different starting geometries for each species (see the Supporting Information, Figure S125), 4 distinct minima for $[\text{Mg}_3\text{Cl}_7]^-$ and 2 for $[\text{Me}_7\text{Mg}_3]^-$ could be identified. In both cases, the global minimum corresponded to an open cubic structure, which was predicted to be significantly lower in energy than the other isomer(s) (Figure 7 and Figure S126 and Table S11 in the Supporting Information).

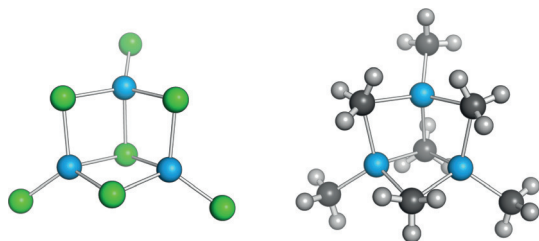


Figure 7. Calculated gas-phase minimum-energy structures for $[\text{Mg}_3\text{Cl}_7]^-$ (left) and $[\text{Me}_7\text{Mg}_3]^-$ (right).

MeMgCl + LiCl

We also used quantum chemical calculations to predict the structures of different minima for the system MeMgCl + LiCl. In the gas phase, the association of the two components results in a heterobimetallic adduct, in which two chlorine atoms bridge the two metal centers. Heterolytic dissociation of this adduct affords the corresponding anionic Mg complex (Figure 8). Essentially the same species are found when solvation by THF is taken into account by using COSMO^[37] and explicitly considering THF molecules to complete the assumed tetrahedral first coordination spheres of the metal ions (see the Supporting Information, Figure S127).

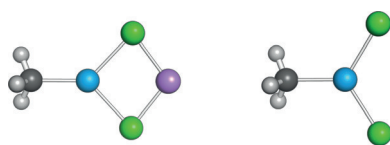


Figure 8. Calculated gas-phase minimum-energy structures for the adduct formed from MeMgCl and LiCl (left) and the anionic complex resulting from its heterolytic dissociation (right).

Discussion

Aggregation state of RMgCl

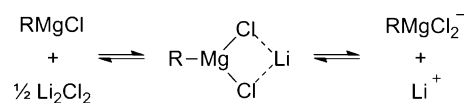
The observation of trinuclear complexes by ESI mass spectrometry disagrees with the presence of mononuclear species inferred from the DOSY measurements. DOSY has recently been established as a standard method for determining the aggregation state of analytes in solution.^[26] Furthermore, the outcome of the DOSY experiments is in accordance with the current consensus on the behavior of Grignard reagents in THF.^[15,16a,b,d,e] Thus, it appears beyond any doubt that the probed RMgCl compounds form mononuclear species in THF. The ECC DOSY measurements afford further information in that they point to the attachment of two molecules of THF to each RMgCl molecule by relating diffusion coefficients to molecular weights. This finding fully matches expectations, because the magnesium center thus reaches its preferred coordination number of 4.

It remains to be clarified why the ESI mass spectrometry experiments arrive at a different result. The ESI process produces small charged droplets, from which the finally observed bare analyte ions are emitted into the gas phase. As the charged droplets rapidly lose solvent molecules due to evaporation, the effective concentration of the analyte increases. This increase may result in a shift of the aggregation equilibria,^[21,43] which can rationalize the observed formation of higher aggregates. Nevertheless, the high specificity of this process and the strong preference for the generation of trinuclear complexes are remarkable. According to the theoretical calculations, the trinuclear anions adopt open cubic structures. This type of structure is closely related to that found for crystals of *i*PrMgCl and *i*PrMgCl-LiCl (Scheme 1)^[19] and can be converted into the latter by the addition of one $[\text{MgX}]^+$ moiety. It thus appears that the ESI process does not form random higher aggregates, but anionic analogues of the species present in the solid state. One might even argue that in this case the ESI process emulates the crystallization process at the molecular level.

For reagents bearing phenyl or 4-anisyl substituents, the ESI-mass spectrometric experiments detected not only trinuclear, but also dinuclear complexes. This finding indicates a special situation for aryl systems.^[44]

Effect of LiCl

The present results consistently indicate that Grignard reagents RMgCl and LiCl react with each other to form ate complexes (Scheme 2).^[45] This reaction involves a 1:1 stoichiometry of both components, as is clearly seen from the electrical conductivity measurements and the Job plot with its maximum at



Scheme 2. Formation of ate complexes from RMgCl and LiCl and their heterolytic dissociation.^[45] Coordinating solvent molecules are omitted for clarity.

$x = 0.5$ for the case of BuMgCl. The quantum-chemical calculations directly show the ate character of the 1:1 adduct, in which the Lewis-acidic Mg center has added the chloro ligand provided by LiCl. Heterolytic dissociation of the contact-ion pair furnishes the free ions detectable by the ESI-mass spectrometric and conductometric experiments (Scheme 2). Thus, our findings qualitatively agree very well with the hypothesis of Krasovskiy, Straub, and Knochel.^[18] Apart from the fact that ate complexes form, it is also of interest to which extent they do so. The formation of trinuclear anions during the ESI process implies that the initially present $[\text{RMgCl}_2]^-$ species find plenty of neutral RMgCl to react with. This apparent abundance of neutral RMgCl can be considered as a first indication for the incomplete formation of ate complexes from RMgCl and LiCl in the sample solutions. Further evidence pointing into this direction comes from the conductivity measurements. The lack of saturation effects, except for the case of *i*PrMgCl, in the titration experiments clearly indicates that the equilibrium between the separated components and the ate complex must lie on the left side for concentrations of $c \approx 250$ mM. Likewise, the relatively broad maximum in the Job plot indicates that the association between BuMgCl and LiCl does not occur quantitatively. As outlined above, the interpretation of the DOSY results depends on the number of THF molecules binding to the $\text{Li}^+[\text{BuMgCl}_2]^-$ complex. As suggested by the quantum chemical calculations, the ate complex binds three THF molecules such that both metal centers are tetrahedrally coordinated. Under this assumption, the DOSY results are also in accordance with an incomplete formation of ate complexes (for $c = 25$ mM).

The present findings can also be compared with our previous results on the related system RZnCl·LiCl.^[25b] For the latter, ate complexes $\text{Li}^+[\text{RZnCl}_2]^-$ form, which are completely analogous to the magnesates observed in the present work. Interestingly, the organozinc halides show a higher tendency to add LiCl than the Grignard reagents ($K_{\text{ass}} \approx 100 \text{ L mol}^{-1}$ for BuZnCl).^[25b] This difference apparently does not reflect simple trends in Lewis acidity, which is higher for Mg^{II} than for Zn^{II}. Possibly, the higher chemical hardness and oxophilicity of the Mg^{II} center favor its interaction with THF as the harder Lewis base, whereas the less hard Zn^{II} center supposedly can better bind chloride as the less hard Lewis base.^[46]

Heterolytic dissociation of RMgCl and $\text{Li}^+[\text{RMgCl}_2]^-$

Both the ESI mass spectrometry experiments and the conductivity measurements show that solutions of Grignard reagents in THF contain ionic species even in the absence of added LiCl. These ions presumably form in an ionic disproportionation [Eq. (4)]. As reported previously, the inferred organomagnesium cations^[20] have so far eluded detection by ESI mass spectrometry because they apparently undergo extremely fast protolysis reactions with traces of protic solvents remaining in the ionization source.^[23c] We have, however, previously observed analogous or similar intact organometallic cations in solutions of organozinc and -indium halides.^[21b, 25b, 47]



The addition of LiCl strongly increases the concentration of free ions in solution because the resulting ate complexes $\text{Li}^+[\text{RMgCl}_2]^-$ can undergo heterolytic dissociation much more easily than simple RMgCl. A very similar situation is found for the related case of RZnCl and $\text{Li}^+[\text{RZnCl}_2]^-$.^[25b] As the conductivity measurements show, the tendency toward dissociation also depends on the nature of the organic substituent. The higher conductivities recorded for the *tert*-butyl system indicate that sterically demanding substituents facilitate heterolytic dissociation. We noted a similar behavior for the cyanocuprates $\text{LiCuR}_2 \cdot \text{LiCN}$.^[25a] An important difference between RMgCl·LiCl and $\text{LiCuR}_2 \cdot \text{LiCN}$ lies in the higher molar conductivities of the latter, which exceed those of the former by one order of magnitude.^[25a] On the basis of the degree of heterolytic dissociation estimated for the cyanocuprates,^[25a] we thus infer that, at synthetically relevant concentrations in THF, at most a few percent of the turbo-Grignard reagents undergo heterolytic dissociation.

Schlenk equilibria

The simultaneous observation of several different $[\text{R}_n\text{Mg}_3\text{Cl}_{7-n}]^-$ ate complexes by ESI mass spectrometry can be viewed as direct evidence for the operation of Schlenk-type equilibria. This finding is in line with previous results.^[15, 16a, b, d, e] Probably, the Schlenk equilibria operate not only in solution, but also in the nanodroplets produced during the ESI process, where the increased analyte concentrations make encounters between individual RMgCl molecules more likely. In comparison to the Grignard reagents bearing primary alkyl groups, those with a secondary or tertiary alkyl substituent apparently had a somewhat lower tendency to undergo exchange reactions and form different $[\text{R}_n\text{Mg}_3\text{Cl}_{7-n}]^-$ ate complexes. Possibly, this deviating behavior is caused by steric effects. In the case of *i*PrMgCl, the addition of dioxane was found to shift the Schlenk equilibrium strongly, thus corroborating earlier reports.^[18]

The failure of the NMR spectroscopic experiments to detect different organomagnesium species even at low temperatures points to high efficiencies of the intermolecular exchange reactions. The occurrence of such exchange reactions was directly proven by the ESI-mass spectrometric detection of mixed complexes upon combination of *i*PrMgCl and PhMgCl. The fact that the detected ate complexes do not show a statistical distribution of the two different organic substituents possibly reflects different ESI activities of the isopropyl- and phenyl-containing magnesium ate complexes.

Reactivity

Taken together, our present results and the previous findings of Knochel and co-workers^[9, 18] point to the in situ-formed magnesates as the reactive component of turbo-Grignard reagents. The present study does not differentiate between contact ion pairs $\text{Li}^+[\text{RMgCl}_2]^-$ and free $[\text{RMgCl}_2]^-$ anions as active species, but the previously reported small effect of added Li^+ -selective

[12]crown-4^[18] suggests that $\text{Li}^+[\text{RMgCl}_2]^-$ and $[\text{RMgCl}_2]^-$ exhibit comparable reactivities in bromine–magnesium exchange reactions. The intermediates formed in these reactions could be directly observed by ESI mass spectrometry. The detected species resemble those found for turbo-Grignard reagents $\text{RMgCl}\cdot\text{LiCl}$ prepared by insertion reactions.

Apart from the synthetically valuable bromine–magnesium exchange reactions, the investigated Grignard reagents and their turbo variants also undergo unwanted decomposition reactions with traces of moisture or oxygen. The propensity toward both reactions strongly depends on the organic substituent of the Grignard reagent. Hydrolysis proceeds particularly quickly for PhMgCl and $\text{PhMgCl}\cdot\text{LiCl}$, but the reason for their enhanced reactivities is unclear. In contrast, oxidation reactions only occur for *i*PrMgCl, *t*BuMgCl, and their turbo counterparts. The higher reactivities of secondary and tertiary alkyl groups indicate the involvement of radicals in these processes.

Finally, the gas-phase fragmentation experiments determined the unimolecular reactivity of the polynuclear organomagnesate anions. The observed loss of organyl-rich neutral fragments resembles the reactions found for other polynuclear organometallic ate complexes.^[21a,b] This fragmentation pattern maximizes the number of electron-withdrawing halogen atoms in the anionic fragments and, thus, helps to stabilize the negative charge.

Comparison of analytical methods

Among the different analytical methods applied in the present work, ESI mass spectrometry provides the most detailed information. This technique affords insight at the strictly molecular level and can, for example, resolve fast Schlenk equilibria. The present work comprises the first successful analysis of intact Grignard reagents by ESI mass spectrometry and thus demonstrates that it can also be successfully applied to the analysis of extremely reactive and sensitive species. However, drawbacks of this method include its limitation to charged analytes and the perturbation introduced by the very nature of the ESI process. As the present findings clearly show, this perturbation can result in drastic shifts of the aggregation equilibria. Furthermore, very weakly bound complexes, such as THF adducts of the magnesium ate anions, do not survive the ESI process (in marked contrast to their more stable cationic analogues).^[23c]

Like ESI mass spectrometry, electrical conductivity measurements only probe the charged components of the sample solution. These measurements do not perturb the analyzed system and, thus, provide direct information on the equilibria operating in solution. A rigorous quantitative analysis of the obtained data is difficult, however, due to the complicating effect of inter-ionic interactions. These interactions are very pronounced for the highly concentrated sample solutions investigated in the present work. Experiments with less concentrated solutions, in turn, would necessarily suffer from an increased degree of unwanted hydrolysis and/or oxidation reactions.

NMR spectroscopy has the advantage of probing analytes irrespective of their charge state. For the problem under investigation, simple one-dimensional NMR spectroscopy proved to be of limited value, however. In contrast, the ECC DOSY method was much more instructive. This technique employs only one internal reference. By using this method and systematically varying the length of the organic substituents in the probed systems, we were able to determine the aggregation states of these systems unambiguously. The same approach also holds promise for the characterization of other analytes by DOSY.

Conclusion

By using a combination of different experimental methods and quantum-chemical calculations, we were able to identify and characterize the molecular constituents of Grignard reagents RMgCl and their turbo variant $\text{RMgCl}\cdot\text{LiCl}$ in ethereal solvents. DOSY measurements of solutions of both reagents in THF showed the presence of complexes containing a single magnesium center. Negative ion-mode ESI mass spectrometry resulted in the detection of trinuclear complexes, which apparently formed due to the concentration increase associated with the ESI process. Quantum chemical calculations suggested that these trinuclear complexes adopt open cubic geometries and, thus, markedly resemble structures previously found for *i*PrMgCl and *i*PrMgCl·LiCl in the solid state. The simultaneous observation of organyl-rich complexes $[\text{R}_n\text{Mg}_3\text{Cl}_{7-n}]^-$ ($n \geq 4$) and organyl-poor ones ($n \leq 3$), moreover directly points to the occurrence of pronounced Schlenk equilibria. The highly dynamic behavior of the organomagnesium species is also reflected in the formation of exchange products upon mixing two different Grignard reagents. ESI mass spectrometry is ideally suited to analyze such processes, as it also unambiguously demonstrated the occurrence of magnesium–bromine exchange reactions upon treatment of a Grignard reagent with an aryl bromide.

The remarkable similarity of the negative ion-mode ESI mass spectra recorded for solutions of conventional Grignard reagents RMgCl on the one hand and for their turbo variant $\text{RMgCl}\cdot\text{LiCl}$ on the other indicates that they do not exhibit significant *qualitative* differences. Both reagents form ate complexes to some extent, which heterolytically dissociate to afford the detected free ions. The degree of magnesate formation and heterolytic dissociation is low for RMgCl and strongly increases upon the addition of LiCl, as revealed by the electrical conductivity measurements. Thus, the two reagents differ at a *quantitative* level. The larger fraction of the more electron-rich and, thus, putatively more nucleophilic ate complexes in the case of the turbo-Grignard reagents explains their enhanced reactivity.

Acknowledgements

We thank Nils Gehrmann, Nico Graw, Hanna Hubrich, Vanessa Reusche, Lucas Weber, and Rahel Ziemer for carrying out some of the conductometric experiments and gratefully acknowl-

edge financial support by the Deutsche Forschungsgemeinschaft (KO 2875/4-1).

Keywords: Grignard reagents • mass spectrometry • NMR spectroscopy • reactive intermediates • salt effect

- [1] V. Grignard, *C. R. Acad. Sci.* **1900**, *130*, 1322–1324.
- [2] D. Seyferth, *Organometallics* **2009**, *28*, 1598–1605.
- [3] M. S. Kharasch, O. Reinmuth, *Grignard Reactions of Nonmetallic Substances*, Prentice-Hall, New York, **1954**.
- [4] K. Oshima in *Science of Synthesis, Vol. 7* (Ed.: H. Yamamoto), Thieme, Stuttgart, **2004**, pp. 573–596.
- [5] a) G. Fouquet, M. Schlosser, *Angew. Chem. Int. Ed. Engl.* **1974**, *13*, 82–83; *Angew. Chem.* **1974**, *86*, 50–51; b) D. Martin, S. Kehrl, M. d'Augustin, H. Clavier, M. Mauduit, A. Alexakis, *J. Am. Chem. Soc.* **2006**, *128*, 8416–8417; c) S. R. Harutyunyan, T. den Hartog, K. Geurts, A. J. Minnaard, B. L. Feringa, *Chem. Rev.* **2008**, *108*, 2824–2852.
- [6] a) M. Tamura, J. K. Kochi, *J. Am. Chem. Soc.* **1971**, *93*, 1487–1489; b) R. J. P. Corriu, J. P. Masse, *J. Chem. Soc. Chem. Commun.* **1972**, 144a; c) K. Tamao, K. Sumitani, M. Kumada, *J. Am. Chem. Soc.* **1972**, *94*, 4374–4376; d) K. Tamao, K. Sumitani, Y. Kiso, M. Zembayashi, A. Fujioka, S.-i. Kodama, I. Nakajima, A. Minato, M. Kumada, *Bull. Chem. Soc. J.* **1976**, *49*, 1958–1969; e) C. E. I. Knappke, A. Jacobi von Wangelin, *Chem. Soc. Rev.* **2011**, *40*, 4948–4962.
- [7] a) R. D. Rieke, P. M. Hudnall, *J. Am. Chem. Soc.* **1972**, *94*, 7178–7179; b) R. D. Rieke, S. E. Bales, *J. Am. Chem. Soc.* **1974**, *96*, 1775–1781; c) T. P. Burns, R. D. Rieke, *J. Org. Chem.* **1987**, *52*, 3674–3680; d) R. D. Rieke, *Science* **1989**, *246*, 1260–1264.
- [8] a) L. Boymond, M. Rottländer, G. Cahiez, P. Knochel, *Angew. Chem. Int. Ed.* **1998**, *37*, 1701–1703; *Angew. Chem.* **1998**, *110*, 1801–1803; b) I. Sapountzis, P. Knochel, *Angew. Chem. Int. Ed.* **2002**, *41*, 1610–1611; *Angew. Chem.* **2002**, *114*, 1680–1681; c) A. E. Jensen, W. Dohle, I. Sapountzis, D. M. Lindsay, V. A. Vu, P. Knochel, *Synthesis* **2002**, 565–569; d) P. Knochel, W. Dohle, N. Gommermann, F. F. Kneisel, F. Kopp, T. Korn, I. Sapountzis, V. A. Vu, *Angew. Chem. Int. Ed.* **2003**, *42*, 4302–4320; *Angew. Chem.* **2003**, *115*, 4438–4456.
- [9] a) A. Krasovskiy, P. Knochel, *Angew. Chem. Int. Ed.* **2004**, *43*, 3333–3336; *Angew. Chem.* **2004**, *116*, 3396–3399; b) F. Kopp, A. Krasovskiy, P. Knochel, *Chem. Commun.* **2004**, 2288–2289; c) H. Ren, A. Krasovskiy, P. Knochel, *Org. Lett.* **2004**, *6*, 4215–4217; d) C. B. Rauhut, V. A. Vu, F. F. Fleming, P. Knochel, *Org. Lett.* **2008**, *10*, 1187–1189; e) N. M. Barl, V. Werner, C. Sämann, P. Knochel, *Heterocycles* **2014**, *88*, 827–844.
- [10] R. L.-Y. Bao, R. Zhao, L. Shi, *Chem. Commun.* **2015**, *51*, 6884–6900. Correction: R. L.-Y. Bao, R. Zhao, L. Shi, *Chem. Commun.* **2015**, *51*, 9744.
- [11] D. Hauk, S. Lang, A. Murso, *Org. Process Res. Dev.* **2006**, *10*, 733–738.
- [12] a) F. M. Piller, P. Appukkuttan, A. Gavryushin, M. Helm, P. Knochel, *Angew. Chem. Int. Ed.* **2008**, *47*, 6802–6806; *Angew. Chem.* **2008**, *120*, 6907–6911; b) F. M. Piller, A. Metzger, M. A. Schade, B. A. Haag, A. Gavryushin, P. Knochel, *Chem. Eur. J.* **2009**, *15*, 7192–7202.
- [13] a) R. E. Mulvey, F. Mongin, M. Uchiyama, Y. Kondo, *Angew. Chem. Int. Ed.* **2007**, *46*, 3802–3824; *Angew. Chem.* **2007**, *119*, 3876–3899; b) E. Hevia, R. E. Mulvey, *Angew. Chem. Int. Ed.* **2011**, *50*, 6448–6450; *Angew. Chem.* **2011**, *123*, 6576–6578; c) B. Haag, M. Mosrin, H. Ila, V. Malakhov, P. Knochel, *Angew. Chem. Int. Ed.* **2011**, *50*, 9794–9824; *Angew. Chem.* **2011**, *123*, 9968–9999; d) A. Harrison-Marchand, F. Mongin, *Chem. Rev.* **2013**, *113*, 7470–7562.
- [14] W. Schlenk, W. Schlenk, Jr., *Ber.* **1929**, *62*, 920–924.
- [15] a) E. C. Ashby, *Q. Rev. Chem. Soc.* **1967**, *21*, 259–285; b) F. W. Walker, E. C. J. Ashby, *J. Am. Chem. Soc.* **1969**, *91*, 3845–3850; c) G. E. Parris, E. C. J. Ashby, *J. Am. Chem. Soc.* **1971**, *93*, 1206–1213; d) E. C. Ashby, *Pure Appl. Chem.* **1980**, *52*, 545–569.
- [16] a) R. M. Salinger, H. S. Mosher, *J. Am. Chem. Soc.* **1964**, *86*, 1782–1786; b) M. B. Smith, W. E. Becker, *Tetrahedron* **1967**, *23*, 4215–4227; c) T. Holm, *Acta Chem. Scand.* **1969**, *23*, 579–586; d) R. Benn, H. Lehmkühl, K. Mehler, A. Ruffínska, *Angew. Chem. Int. Ed. Engl.* **1984**, *23*, 534–535; *Angew. Chem.* **1984**, *96*, 521–523; e) T. S. Ertel, H. Bertagnolli, *Polyhedron* **1993**, *12*, 2175–2184.
- [17] a) P. Jolibois, *Compt. Rend.* **1912**, *155*, 353–355; b) W. V. Evans, R. Pearson, *J. Am. Chem. Soc.* **1942**, *64*, 2865–2871; c) R. E. Dessy, R. M. Jones, *J. Org. Chem.* **1959**, *24*, 1685–1689.
- [18] A. Krasovskiy, B. F. Straub, P. Knochel, *Angew. Chem. Int. Ed.* **2006**, *45*, 159–162; *Angew. Chem.* **2006**, *118*, 165–169.
- [19] F. Blasberg, M. Bolte, M. Wagner, H.-W. Lerner, *Organometallics* **2012**, *31*, 1001–1005.
- [20] For examples of a structurally characterized anionic trisorganyl magnesium ate complex and an organomagnesium cation, see: C. Lichtenberg, T. P. Spaniol, I. Peckermann, T. P. Hanusa, J. Okuda, *J. Am. Chem. Soc.* **2013**, *135*, 811–821.
- [21] a) K. Koszinowski, P. Böhrer, *Organometallics* **2009**, *28*, 100–110; b) K. Koszinowski, *J. Am. Chem. Soc.* **2010**, *132*, 6032–6040; c) A. Putau, H. Brand, K. Koszinowski, *J. Am. Chem. Soc.* **2012**, *134*, 613–622; d) T. D. Blümke, T. Klatt, K. Koszinowski, P. Knochel, *Angew. Chem. Int. Ed.* **2012**, *51*, 9926–9930; *Angew. Chem.* **2012**, *124*, 10064–10068.
- [22] a) B. H. Lipshutz, K. L. Stevens, B. James, J. G. Pavlovich, *J. Am. Chem. Soc.* **1996**, *118*, 6796–6797; b) B. H. Lipshutz, J. Keith, D. J. Buzard, *Organometallics* **1999**, *18*, 1571–1574; c) M. A. Henderson, T. K. Trefz, S. Collins, M. Y. Wang, J. S. McIndoe, *Organometallics* **2013**, *32*, 2079–2083; d) T. K. Trefz, M. A. Henderson, M. Y. Wang, S. Collins, J. S. McIndoe, *Organometallics* **2013**, *32*, 3149–3152; e) T. K. Trefz, M. A. Henderson, M. Linnolahti, S. Collins, J. S. McIndoe, *Chem. Eur. J.* **2015**, *21*, 2980–2991.
- [23] a) S. Sakamoto, T. Imamoto, K. Yamaguchi, *Org. Lett.* **2001**, *3*, 1793–1795; b) M. A. Schade, J. E. Fleckenstein, P. Knochel, K. Koszinowski, *J. Org. Chem.* **2010**, *75*, 6848–6857; c) C. Schnegelsberg, T. D. Blümke, K. Koszinowski, *J. Mass Spectrom.* **2015**, *50*, 1393–1395.
- [24] To avoid the difficulties associated with the direct analysis of organomagnesium ions by ESI mass spectrometry, O'Hair and co-workers developed an elegant gas-phase synthesis of these species: a) R. A. J. O'Hair, A. K. Vrkic, P. F. James, *J. Am. Chem. Soc.* **2004**, *126*, 12173–12183; b) G. N. Khairallah, C. Thum, R. A. J. O'Hair, *Organometallics* **2009**, *28*, 5002–5011; c) G. N. Khairallah, E. J. H. Yoo, R. A. J. O'Hair, *Organometallics* **2010**, *29*, 1238–1245; d) M. G. Leeming, G. N. Khairallah, G. da Silva, R. A. J. O'Hair, *Organometallics* **2011**, *30*, 4297–4307; e) G. N. Khairallah, C. C. L. Thum, D. Lesage, J.-C. Tabet, R. A. J. O'Hair, *Organometallics* **2013**, *32*, 2319–2328.
- [25] a) A. Putau, K. Koszinowski, *Organometallics* **2011**, *30*, 4771–4778; b) J. E. Fleckenstein, K. Koszinowski, *Organometallics* **2011**, *30*, 5018–5026.
- [26] a) D. Li, I. Keresztes, R. Hopson, P. G. Williard, *Acc. Chem. Res.* **2009**, *42*, 270–280; b) G. Kagan, W. Li, R. Hopson, P. G. Williard, *Org. Lett.* **2010**, *12*, 520–523; c) D. R. Armstrong, P. García-Álvarez, A. R. Kennedy, R. E. Mulvey, J. A. Parkinson, *Angew. Chem. Int. Ed.* **2010**, *49*, 3185–3188; *Angew. Chem.* **2010**, *122*, 3253–3256; d) D. R. Armstrong, W. Clegg, P. García-Álvarez, M. D. McCall, L. Nuttall, A. R. Kennedy, L. Russo, E. Hevia, *Chem. Eur. J.* **2011**, *17*, 4470–4479; e) P. García-Álvarez, R. E. Mulvey, J. A. Parkinson, *Angew. Chem. Int. Ed.* **2011**, *50*, 9668–9671; *Angew. Chem.* **2011**, *123*, 9842–9845; f) A.-C. Pöpppler, M. M. Meinholz, H. Faßhuber, A. Lange, M. John, D. Stalke, *Organometallics* **2012**, *31*, 42–45; g) A. Hernán-Gómez, E. Herd, E. Hevia, A. R. Kennedy, P. Knochel, K. Koszinowski, S. M. Manolikakes, R. E. Mulvey, C. Schnegelsberg, *Angew. Chem. Int. Ed.* **2014**, *53*, 2706–2710; *Angew. Chem.* **2014**, *126*, 2744–2748; h) R. Neufeld, D. Stalke, *Chem. Sci.* **2015**, *6*, 3354–3364; i) R. Neufeld, M. John, D. Stalke, *Angew. Chem. Int. Ed.* **2015**, *54*, 6994–6998; *Angew. Chem.* **2015**, *127*, 7100–7104.
- [27] A. Krasovskiy, P. Knochel, *Synthesis* **2006**, 5, 890–891.
- [28] A. Putau, K. Koszinowski, *Organometallics* **2010**, *29*, 3593–3601; Addition/Correction: A. Putau, K. Koszinowski, *Organometallics* **2010**, *29*, 6841–6842.
- [29] K. Koszinowski, F. Lissy, *Int. J. Mass Spectrom.* **2013**, *354/355*, 219–228.
- [30] a) A. Jerschow, N. Müller, *J. Magn. Reson.* **1997**, *125*, 372–375; b) A. Jerschow, N. Müller, *J. Magn. Reson. Ser. A* **1996**, *123*, 222–225.
- [31] F. Neese, *WIREs Comput. Mol. Sci.* **2012**, *2*, 73–78.
- [32] F. Neese, *ORCA—An ab initio, DFT and semiempirical SCF-MO Package, Version 3.0.3*, Max-Planck-Institute for Chemical Energy Conversion, **2013**.
- [33] a) A. D. Becke, *J. Chem. Phys.* **1993**, *98*, 5648–5652; b) P. J. Stephens, F. J. Devlin, C. F. Chabalowski, M. J. Frisch, *J. Phys. Chem.* **1994**, *98*, 11623–11627.

- [34] a) S. Grimme, J. Antony, S. Ehrlich, H. Krieg, *J. Chem. Phys.* **2010**, *132*, 154104; b) S. Grimme, S. Ehrlich, L. Goerigk, *J. Comput. Chem.* **2011**, *32*, 1456–1465.
- [35] F. Weigend, R. Ahlrichs, *Phys. Chem. Chem. Phys.* **2005**, *7*, 3297–3305.
- [36] J. Zheng, X. Xu, D. G. Truhlar, *Theor. Chem. Acc.* **2011**, *128*, 295–305.
- [37] a) A. Klamt, G. Schüürmann, *J. Chem. Soc. Perkin Trans. 2* **1993**, 799–805; b) S. Sinnecker, A. Rajendran, A. Klamt, M. Diedenhofen, F. Neese, *J. Phys. Chem. A* **2006**, *110*, 2235–2245.
- [38] G. Sosnovsky, J. H. Brown, *Chem. Rev.* **1966**, *66*, 529–566.
- [39] No gas-phase fragmentation experiments were performed for $[\text{Et}_n\text{Mg}_3\text{Cl}_{7-n}]^-$ because extensive overlaps between the isotopologues of different ions prevented a meaningful mass selection and analysis.
- [40] a) M. Hojo, T. Ueda, Z. Chen, M. Nishimura, *J. Electroanal. Chem.* **1999**, *468*, 110–116; b) D. Das, *J. Solution Chem.* **2008**, *37*, 947–955.
- [41] J. S. Renny, L. L. Tomasevich, E. H. Tallmadge, D. B. Collum, *Angew. Chem. Int. Ed.* **2013**, *52*, 11998–12013; *Angew. Chem.* **2013**, *125*, 12218–12234.
- [42] The determined value only corresponds to a lower value because the associated molar van der Waals density of $\text{BuMgCl}\cdot\text{LiCl}\cdot 2\text{THF}$ exceeds the recommended limit for the determination of exact MW_{det} values (see the Supporting Information).
- [43] N. G. Tsierkezos, J. Roithová, D. Schröder, M. Ončák, P. Slaviček, *Inorg. Chem.* **2009**, *48*, 6287–6296.
- [44] In the case of PhMgCl , their partial hydrolysis and the ability of the resulting OH groups to form hydrogen bonds could, however, possibly also favor the formation of dinuclear complexes.
- [45] LiCl is known to be present as dimeric Li_2Cl_2 in THF: a) M. K. Wong, A. I. Popov, *J. Inorg. Nucl. Chem.* **1972**, *34*, 3615–3622; b) H. J. Reich, J. P. Borst, R. R. Dykstra, P. D. Green, *J. Am. Chem. Soc.* **1993**, *115*, 8728–8741.
- [46] R. G. Pearson, *J. Am. Chem. Soc.* **1963**, *85*, 3533–3539.
- [47] J. E. Fleckenstein, K. Koszinowski, *Chem. Eur. J.* **2009**, *15*, 12745–12753.

Received: February 15, 2016

Published online on May 6, 2016